



HAL
open science

Characterization of Silica Gels by ^{29}Si MAS NMR and IR Spectroscopic Measurements

Wolfgang Lutz, Dirk Täschner, Rolf Kurzhals, Detlef Heidemann, Cornelia Hübert

► **To cite this version:**

Wolfgang Lutz, Dirk Täschner, Rolf Kurzhals, Detlef Heidemann, Cornelia Hübert. Characterization of Silica Gels by ^{29}Si MAS NMR and IR Spectroscopic Measurements. *Journal of Inorganic and General Chemistry / Zeitschrift für anorganische und allgemeine Chemie*, 2009, 635 (13-14), pp.2191. 10.1002/zaac.200900237 . hal-00509231

HAL Id: hal-00509231

<https://hal.science/hal-00509231>

Submitted on 11 Aug 2010

HAL is a multi-disciplinary open access archive for the deposit and dissemination of scientific research documents, whether they are published or not. The documents may come from teaching and research institutions in France or abroad, or from public or private research centers.

L'archive ouverte pluridisciplinaire **HAL**, est destinée au dépôt et à la diffusion de documents scientifiques de niveau recherche, publiés ou non, émanant des établissements d'enseignement et de recherche français ou étrangers, des laboratoires publics ou privés.



Characterization of Silica Gels by ^{29}Si MAS NMR and IR Spectroscopic Measurements

Journal:	<i>Zeitschrift für Anorganische und Allgemeine Chemie</i>
Manuscript ID:	zaac.200900237.R1
Wiley - Manuscript type:	Article
Date Submitted by the Author:	08-Jun-2009
Complete List of Authors:	Lutz, Wolfgang; Süd-Chemie Zeolites GmbH Täschner, Dirk; Süd-Chemie Zeolites GmbH Kurzhaus, Rolf; Süd-chemie Zeolites GmbH Heidemann, Detlef; Humboldt-Universität Hübert, Cornelia; Brandenburgisch Technische Universität
Keywords:	silicates, solid state structure, solvent effects, NMR spectroscopy, IR spectroscopy



1
2
3
4
5
6
7
8 Characterization of silica gels by ^{29}Si MAS NMR and IR spectroscopic
9
10 measurements
11

12
13 W. Lutz*, D. Täschner, R. Kurzhals, ¹D. Heidemann, ²C. Hübert,
14

15
16 Berlin and Bitterfeld, Süd-Chemie Zeolites GmbH,
17

18 ¹Berlin, Humboldt-Universität zu Berlin
19

20 ²Cottbus, Brandenburgische Technische Universität
21

22
23 Received

24
25
26
27 **Abstract**
28

29 The solubility of commercial and synthesized silica gels in a solution of Tetra-Ethyl-
30 Ammonium-Hydroxide (TEAOH) was investigated at room temperature. The state of parent
31 silica frameworks was characterized by BET and SEM. The structural defects were identified
32 both by the Q^n group analysis in ^{29}Si MAS NMR and IR spectroscopic investigation. It was
33 found that the dissolution rate of the samples shows a tendency for growing up with an
34 increasing BET surface. The increase of the internal surface was accompanied by formation of
35 $\text{Si}(\text{OSi})_3(\text{OH})$ (Q^3) and $\text{Si}(\text{OSi})_2(\text{OH})_2$ (Q^2) structural units. The higher the number of Q^3 and
36 Q^2 groups observed, the faster the samples were dissolved in TEAOH solution due to the
37 attack of the hydroxide ions on the terminal OH groups of the framework. The asymmetrical
38 TOT valence vibration of the IR spectra was systematically shifted to lower values with
39 increase in the number of Q^3 and Q^2 structure groups.
40
41
42
43
44
45
46
47
48
49
50
51
52

53 **Keywords:** silica gel, preparation, solubility, ^{29}Si MAS NMR and IR spectroscopy
54
55

56
57 * Wolfgang Lutz

58 Süd-Chemie Zeolites GmbH, Labor Berlin, Volmerstr. 13, 12489 Berlin

59 Tel.: 0049 30 6392 4425

60 e-mail: wolfgang.lutz@sud-chemie.com

1
2
3
4
5
6 Charakterisierung von Silicagelen mit Hilfe der IR- and ^{29}Si MAS NMR-
7
8
9 Spektroskopie
10
11
12
13

14
15 **Inhaltsübersicht.**
16

17 Die Löslichkeit kommerzieller Silicagele und Gele eigener Herstellung in TEAOH-Lösung
18 wurde bei Raumtemperatur untersucht. Die Löslichkeit stieg mit zunehmender Zahl von
19
20 Strukturdefekten in der SiO_2 -Matrix, die mit Hilfe der Q^n -Gruppen-Analyse aus ^{29}Si MAS
21
22 NMR-Spektren charakterisiert wurden. Die Wellenzahl der asymmetrische TOT (T = Si)
23
24 Valenzschwingung in IR-Spektren verschob sich mit Zunahme der Strukturdefekte
25
26 systematisch zu niedrigeren Werten.
27
28
29
30
31
32
33
34
35
36
37
38
39
40
41
42
43
44
45
46
47
48
49
50
51
52
53
54
55
56
57
58
59
60

1 Introduction

Silica gels have been used in the chemical industry and laboratory technique as drying agents [1], feed stock of zeolite synthesis [2], and separation medium in chromatography [3] for a long period. More recently, they were applied also as wafer of optical sensors [4] and for heat storage by water sorption [5]. Pioneers reporting the physical and chemical properties of silica gels are Hauser [6], Sosman [7], or Hinz [8]. A general view about “The chemistry of silica” was published in 1979 by Iler [9].

Engelhardt and Michel [10] characterized the framework of silica gels by the Q^n group analysis (n = number of bridging oxygen atoms in the SiO_4 -tetrahedron under study) and Cannes [11] reported on the surface properties by the characterization of silanol groups by means of ^{29}Si MAS NMR and CP MAS NMR experiments. IR spectroscopic measurements gave information about surface OH-groups [11, 12] and the SiO_2 framework [13].

The application of silica gels for the synthesis of zeolites was described in detail by Breck [1], Barrer [2], and Zhdanov [14]. The synthesis process of these aluminosilicates follows quite different recipes. The particle size, size distribution, and shape of the crystals obtained are decisively determined by the crystallization kinetics. All parameters depend on the temperature, alkalinity and composition of the synthesis batch, and, finally, the type of silica source. While in the classical synthesis of 4A (LTA) and X (FAU) zeolites water glass solution is used as silicate component, the synthesis of zeolites beta (BEA), mordenite (MOR), or ZSM-5 (MFI) involves the silica gels.

The reactivity of silica gels depends on their solubility in the alkaline mother liquors of the synthesis batches. Mechanism, kinetics and, consequently, the quality of the final products are thereby influenced by the size of SiO_2 particles as well as by the condensation state of the SiO_2 network. The crystal shape can be characterized by the scanning electron microscopic

1
2
3 investigation (SEM) and the solubility by chemical analysis of the liquid phase. ^{29}Si MAS
4
5 NMR and IR measurements can give direct hints to the state of the SiO_2 framework.
6
7

8 This paper is aimed to demonstrate the applicability of the ^{29}Si MAS NMR as well as the IR
9
10 spectroscopy as suitable methods for the efficient characterization of the framework state of
11
12 silica gels, using two differently prepared sample series.
13
14
15
16
17
18
19
20
21
22
23
24
25
26
27
28
29
30
31
32
33
34
35
36
37
38
39
40
41
42
43
44
45
46
47
48
49
50
51
52
53
54
55
56
57
58
59
60

2 Experimental

Materials

Commercial silica gels used for different zeolite synthesis processes and shown in Tab. 1 as well as synthesized silica gels were investigated. The latter were prepared according to the following route. The aqueous solution of sodium silicate was transformed into acid silica sol using “Wofatit KPS 200” as ion exchanger resin. 220 ml silicate solution (1.8 M in SiO₂) was dropped into a stirred batch of 1000 ml resin and 200 ml water at 278 K within 10 minutes. The acidity of the as-synthesized silica sol with pH of 2 was adjusted to pH values between 3 and 8 by immediate adding of sodium hydroxide solution. SiO₂ xerogels were obtained by drying of the washed hydrogels at 383 K for 24 hours and subsequent crushing.

Solubility experiments

1 g silica gel was stirred at ambient temperature in 40 ml of a 15% aqueous solution of TEAOH for 15 – 60 minutes. Before ICP OES element analysis, the solution was separated from the solid by filtration over glass micro filters MF 100 (Fisherbrand) in a first step followed by the filtration using PTFE micro-membrans (0.2 μm) under pressure within 5 minutes. The separation period was part of the total treatment time. The solubility of the glass filter material does not exceed 3 mg/l and can be, therefore, neglected. Cellulose membranes were non-suitable for the separation procedure because the material dissolves itself under these conditions.

The filtrates were analyzed by use of a IRIS Intrepid High Resolution spectrometer (Thermo Elemental, USA). The ICP OES was calibrated within reference to synthesized solution standards. The accuracy of the measurements lies around 1-3 % within relative standard deviation (RSD) for values above background equivalent concentration (BEC).

Characterization of xerogels

The ^{29}Si MAS NMR spectra were recorded at room temperature on a Bruker Avance 400 spectrometer, operating at frequencies of 79.5 MHz. A 4 mm double tuned (^1H -X) MAS probe (Bruker Biospin) was used to perform MAS NMR measurements at spinning rates of 12 kHz. The spectra were obtained with a single pulse excitation consisting of 4 μs pulses ($\pi/2$ pulses) and recycle delays of 120 seconds to exclude saturation effects. Up to 700 FIDs were accumulated to obtain reliable signal-to-noise ratio. The spectra were externally referenced to liquid Me_4Si at 0 ppm. A detailed Q^n -group characterization includes the line shape analysis of the NMR spectra by use of an iterative deconvolution procedure with the help of dmfit software package [15].

IR absorption spectra were taken on a Shimadzu FTIR 8400S spectrometer with a resolution of $\pm 1 \text{ cm}^{-1}$ by use of 30 scans. For analysis, 0.5 mg of the sample was pressed with 400 mg KBr into a pellet and measured in the IR range of 400 cm^{-1} to 4000 cm^{-1} .

Scanning electron microscopy (SEM) was performed on a Hitachi S2400 with W cathode at the accelerating potential of 15-20 kV. To produce the conductive layer, the particles were sputtered by a thin gold coating.

Chemical element analysis was measured by using XRF spectrometer PW2404 from Panalytical. 0,5 g of the sample were fused with 3 g lithium borate ($\text{Li}_4\text{B}_6\text{O}_{11}$, Spectromelt A12 from Merck GmbH) in a platinum crucible to cast a 27 mm diameter glass disc.

The BET surface area was determined on basis of the volumetric nitrogen adsorption at $p/p_0 = 0.075, 0.1, \text{ and } 0.125$ at -77.8 K on a Nova 1200 of the Quantachrome Corporation.

Results and discussion

The commercial and synthesized silica gels listed in Tab. 1 show similar dissolution behaviour in the TEAOH solution. The amounts of dissolved SiO₂ vary between 50 und 800 mg/l in dependence on time and sample type for both series (Figs. 1 and 2). The dissolution rate increases thereby with the absolute rising solubility of samples.

The kinetic curves of the commercial products given in Fig. 1 show higher concentrations of dissolved SiO₂ for Promeksil B12, Aerosil 200, and Sipernat 320 connected with the transformation of the solids into transparent hydrogels according to visual observation, while Silica 995 and Aerosil OX 50 show lower dissolution degree, with a formation of SiO₂ nanoparticles.

The curves of the synthesized gels in Fig. 2 demonstrate increasing dissolution with decreasing pH-values of preparation. The remaining filter cakes of this series represent white gels for all the samples.

SEM micrographs of the commercial products provide the evidence that they are composed of primary particles with a significant surface roughness. In this case, particle size distribution is broad. In contrast, the synthesized samples have somewhat greater particles with a rather smooth surface. Their size lies between 10 and 910 μm (Tab. 1). Selected replicas of both series are shown in Fig. 3.

As it can be seen from Tab. 1 and Fig. 3, the particle size and the crystal shape do not influence the solubility of the gels in a systematic way. The reason consists in the fact that the size distribution of the primary particles is more uniform and does not differ in less than 0.1 μm for all samples (Tab. 1).

In opposite to the values of the secondary particle size, the BET surface of samples show a systematic change and coincides with the trend in solubility. Whereas the BET values of the commercial products vary between 42 and 413 m²/g, the surface of the synthesized silica gels

1
2
3 ranges from 140 to 438m²/g as shown in Tab. 1. As evident from Figs. 1 and 2, the amount of
4 dissolved SiO₂ of the Aerosil OX 50 and SiO₂ (pH=8) is consequently lowest and for
5 Promeksil B12 and SiO₂(pH=4) this parameter is observed as being highest. But in spite of the
6
7
8
9
10
11
12
13
14
15
16
17
18
19
20
21
22
23
24
25
26
27
28
29
30
31
32
33
34
35
36
37
38
39
40
41
42
43
44
45
46
47
48
49
50
51
52
53
54
55
56
57
58
59
60

ranges from 140 to 438m²/g as shown in Tab. 1. As evident from Figs. 1 and 2, the amount of dissolved SiO₂ of the Aerosil OX 50 and SiO₂ (pH=8) is consequently lowest and for Promeksil B12 and SiO₂(pH=4) this parameter is observed as being highest. But in spite of the somewhat higher BET surface of the synthesized gels, their solubility does not reach higher values. For understanding of this phenomenon, the structure of the gel frameworks must be taken into consideration in more details.

The Qⁿ-group analysis on basis of the ²⁹Si MAS NMR spectroscopic measurements confirmed the dependence of the gel solubility on the state of the silica framework and, thus the structure of the internal surface. The NMR spectra of the commercial silica gels (see Fig. 4) normalized to 100% intensity show different line shape and chemical shifts of the peaks: Promeksil B12 and Sipernat 320 are characterized by different kinds of Qⁿ-signals. Firstly, there is Q⁴ the main signal related to each Si atom which is linked over oxygen atoms with 4 Si neighbours. Additional signals such as Q³ and Q² are also present in this spectrum. The first and the second are coming from 3 Si neighbours and 1 OH-group and 2 Si neighbours and 2 OH-groups, respectively. The chemical shift of the Q⁴-peak appears at about -110 ppm and that of the Q³-peaks is observed at -100 ppm. These values of chemical shift are near to those known for cristobalite rather than to tridymite or quartz. Only the Q²-peaks strongly differ with values of -92,4 ppm and -95,3 ppm for Promeksil B12 and Sipernat 320, respectively. While the Q⁴-groups characterize network with a perfect structure consisting of SiO₄-tetrahedrons, the Q³- and Q²-groups characterize an imperfect framework responsible for the formation of chemically active hydroxyl groups. In this consequence, commercial Aerosil 200, Silica 995 and Aerosil OX 50 contain only Q³-groups related to defects in decreasing extent. However, their peak width is relative broad in comparison with crystalline silicate phases such as quartz, tridymite, and cristobalite because of non-perfect bond length and angles of their structural polyhedra.

1
2
3 For all the samples except Sipernat 320, the gel solubility increases with the rising degree of
4 defects. In contrast to Silica 995, Sipernat 320 seems to be less soluble although it contains
5 quite more defects. The reason could be associated with a relative high content of Na₂O of 2.1
6 weight-% (see Tab. 1) and especially contaminants of 0.15 weight-% Al₂O₃ which remarkably
7 reduce the amount of dissolved of SiO₂. Sodium silicate and sodium aluminate which are
8 formed under action of the TEAOH solution lead to a stronger condensation of (SiO₂)_n units
9 over -Si-O-Al-O-Si- bonds. Sipernat 320 produces, therefore, more hydrogel gel than Aerosil
10 200 and Promeksil B12.
11
12

13
14
15 As evident from Fig. 5, ²⁹Si MAS NMR spectra of the synthesized samples show Q⁴-groups
16 as well as Q³ and Q²-groups. The corresponding signals are centred at similar chemical shifts
17 of about -111 ppm (Q⁴), -101 ppm (Q³), and -92-93 ppm (Q²) as in the case of commercial
18 products. But the line width of the signals observed are smaller. This could give a hint to the
19 higher regularity in respect to the bond length and angle. This may compensate the greater
20 number of defects which affect the dissolution behaviour, therefore the solubility becomes
21 smaller than expected from the BET surface values.
22
23

24
25
26 IR spectroscopic measurements give also a direct hint to the state of the SiO₂ framework. For
27 two selected samples, typical spectra are shown in Fig. 6. One could recognise peaks for the
28 tetrahedron, the symmetrical TOT valence, and the asymmetrical TOT valence vibration in the
29 range of wave numbers of 467-478 cm⁻¹, 802-812 cm⁻¹, and 1082-1121 cm⁻¹, respectively.
30 Particularly, the asymmetrical TOT (T=Si) valence vibration shifts significantly to lower w_{TOT}
31 values with a raising number of the framework defects as it is shown in Tab. 1.
32
33

34
35
36 This effect was extensively investigated for aluminosilicate zeolites, e.g. of the Y type [16,
37 17]. With change in the content of framework aluminium in Si/Al ratios from 2.4 to 139, w_{TOT}
38 peak shifts from 1019 to 1082 cm⁻¹ [18]. The reason could be in more regular bond angles
39 when aluminium content is decreased owing to different bond length of the Al-O and the Si-O
40
41
42
43
44
45
46
47
48
49
50
51
52
53
54
55
56
57
58
59
60

1
2
3 units with 173 pm and 163 pm, respectively. A pure SiO₂ framework needs therefore higher
4
5 activation energy for the vibrations which reflects in a higher wave number during IR
6
7 spectroscopic measurements.
8
9

10 Although silica gels practically do not contain aluminium atoms, the shift of the TOT valence
11
12 vibration depends also on the different bond length and angle in Si(OSi)₄, Si(OSi)₃(OH) or
13
14 Si(OSi)₂(OH)₂ tetrahedra. In contrast to the synthesized samples, the w_{TOT} values of the
15
16 commercial silica gels are generally slightly higher and differ, with values ranging from 1101
17
18 to 1120 cm⁻¹ against values lying between 1082 and 1105 cm⁻¹. It means that commercial
19
20 products have low degree of defects which fits nicely with data obtained by the ²⁹Si MAS
21
22 NMR spectra. This is the reason why Aerosil OX 50 or SiO₂(pH=8) needs the highest and
23
24 Promexsil B12 and SiO₂(pH=2) the lowest activation energies corresponding to the highest
25
26 and the lowest IR wave numbers for each series as seen from Tab. 1. The solubility of the
27
28 samples increases in the same tendency.
29
30
31
32
33

34 In the series of synthesized silica gels, a specific observation lies in the fact that the saturation
35
36 of w_{TOT} begins with pH value equal to 6. In this range, the ²⁹Si MAS NMR is more sensitive
37
38 than the IR spectroscopy. Nevertheless, synthesized silica gel products could be characterized
39
40 by IR spectroscopic measurements with a high sensitivity over a wide range, too.
41
42
43
44
45
46
47
48
49
50
51
52
53
54
55
56
57
58
59
60

Conclusion

The solubility of silica gels in TEAOH solution depends on the internal BET surface of samples. In opposite to crystalline porous silicates such as zeolites, the surface of silica gels with irregular pore system contains, in addition to $\text{Si}(\text{OSi})_4$ (Q^4), $\text{Si}(\text{OSi})_3\text{OH}$ (Q^3) and $\text{Si}(\text{OSi})_2(\text{OH})_2$ (Q^2) structure units. The more the SiO_2 framework is disturbed, the stronger hydroxide ions of the TEAOH solution attack the silica framework at the terminal OH groups.

In the case of commercial products, manufacturing process affects the formation of structural defects and cannot be exactly estimated. In the case of silica gels which were obtained from precipitation on basis of water glass solution (synthesized samples), it was observed that the number of defects increases with decreasing the pH value during precipitation process.

The Q^n group analysis of the silica gels was successfully employed with the help of ^{29}Si MAS NMR measurements. It appeared also that IR spectroscopic analysis could help with the reliable characterization of the structure under special consideration. In this case, the asymmetrical TOT valence vibration of the SiO_2 framework shifts sensitively to lower wave numbers with the raising degree of defects.

The shape of the secondary silica gel particles, characterized by SEM, does not influence the dissolution systematically. Different residual filter cakes such as white solids, transparent hydro-gels, and silica nano-particles can be observed. The contamination of the silica gel by traces of aluminium compounds leads to the increased formation of a secondary gel phase due to precipitation of the secondary $(\text{SiO})_n$ particles containing -Si-O-Al-O-Si- bonds.

References

- [1] D.W. Breck, *Zeolite Molecular Sieves*, John Wiley & Sons, London 1974.
- [2] R. Barrer, *Hydrothermal Chemistry of Zeolites*, Academic Press, London, 1982.
- [3] Chromatographie
- [4] C. Mc Donagh, P. Bowe, K. Mongey, B. D. Mac Craith, *J. Non-Cryst. Solids*, **2002**, 306, 138.
- [5] A.O. Dieng, R.Z. Wang, *Renew. Sustainable Energy Rev.*, **2001**, 5, 313.
- [6] E. H. Hauser, *Silicic Science*, Van Nostrand, Princeton, 1955.
- [7] R. B. Sosman, *The Phase of Silica*, Rutgers University Press, New Brunswick, 1965.
- [8] W. Hinz, *Silicate: Grundlagen der Silicatwissenschaft und Silicattechnik*, Vol. 2, Verlag Bauwesen, Berlin, 1971.
- [9] R.K. Iler, *The chemistry of silica*, Wiley & Sons, New York, 1979.
- [10] G. Engelhardt, D. Michel, *High Resolution Solid State NMR of Silicates and Zeolites*, Wiley & Sons, New York, 1987.
- [11] C. Cannas, M. Casu, A. Musinu, G. Piccaluga, *J. Non-Cryst. Solids*, **2005**, 351, 3476.
- [12] J. Estella, J. C. Echeverria, M. Laguna, J. Garrido, *Microp. Mesopor. Mater.*, **2007**, 102, 274.
- [13] A. Fidalgo, L. M. Ilharco, *Microp. Mesopor. Mater.*, **2005**, 84, 229.
- [14] S.P. Zhdanov, S.S. Chvoshchev, N.N. Samulevich, *Synthesized Zeolites*, Gordon & Breach Science Publishers, New York, 1990.
- [15] D. Massiot, F. Fayon, M. Capron, I. King, S. Le Calvé, B. Alonso, J.O. Durand, B. Bujoli, Z. Gan, G. Hoatson, *Magn. Reson. Chem.* 40 (2002) 70 - 76
- [16] E. M. Flanigen, in *Zeolite Chem. Catal.* Ed. J. A. Rabo, ACS Monographs 171 (1976) 81.
- [17] H. Fichtner-Schmittler, U. Lohse, H. Miessner, H. E. Maneck, *Z. Phys. Chem.*

1
2
3 Leipzig 271 (1990) 69.
4

- 5 [18] C. H. Rüscher, J.-Chr. Buhl, W. Lutz, in A. Galarneau, F. Di Renzo, F. Fajula, and
6 J. Vedrine (Eds.), *Stud. Surf. Sci. Cat.*, Vol. 135, Elsevier, Amsterdam, 2001, 13-P15,
7
8 p. 1.
9
10
11
12
13
14
15
16
17
18
19
20
21
22
23
24
25
26
27
28
29
30
31
32
33
34
35
36
37
38
39
40
41
42
43
44
45
46
47
48
49
50
51
52
53
54
55
56
57
58
59
60

Table 1

sample denotation	sample type	particle size μm secondary/primary	BET surface m^2/g	IR ν_{TOT} , cm^{-1}
<i>commercial silica gels</i>				
Promeksil B12	precipitated	< 10 / < 0.08	413	1101
Sipernat 320	precipitated	< 75 / < 0.06	196	1107
Aerosil 200	pyrogene	< 310 / < 0.09	210	1110
Silica 995	pyrogene	< 28 / < 0.07	61	1117
Aerosil OX 50	pyrogene	< 34 / < 0.09	42	1120
<i>synthesized silica gels</i>				
SiO ₂ (pH 2)	precipitated	< 380 / < 0.12	538	1082
SiO ₂ (pH 3)	precipitated	< 283 / < 0.08	513	1088
SiO ₂ (pH 4)	precipitated	< 103 / < 0.09	507	1095
SiO ₂ (pH 5)	precipitated	< 94 / < 0.03	404	1101
SiO ₂ (pH 6)	precipitated	< 112 / < 0.06	352	1105
SiO ₂ (pH 7)	precipitated	< 910 / < 0.04	172	1103
SiO ₂ (pH 8)	precipitated	< 113 / < 0.06	140	1105

Fig. 1 Alkaline solubility of commercial silica gels

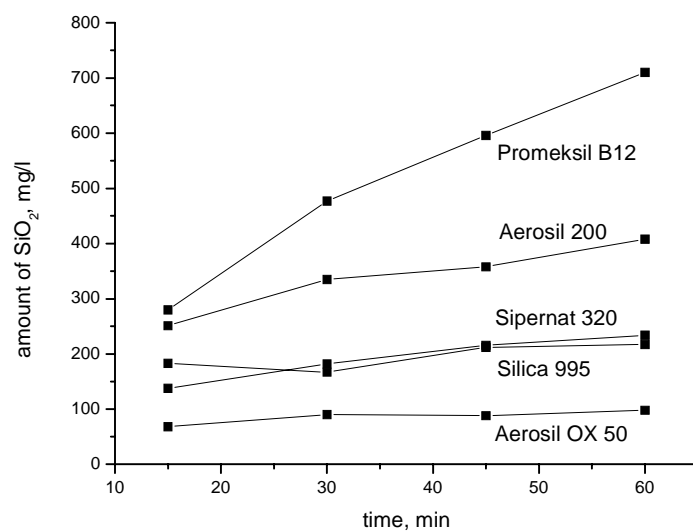


Fig. 2 Alkaline solubility of synthesized silica gels

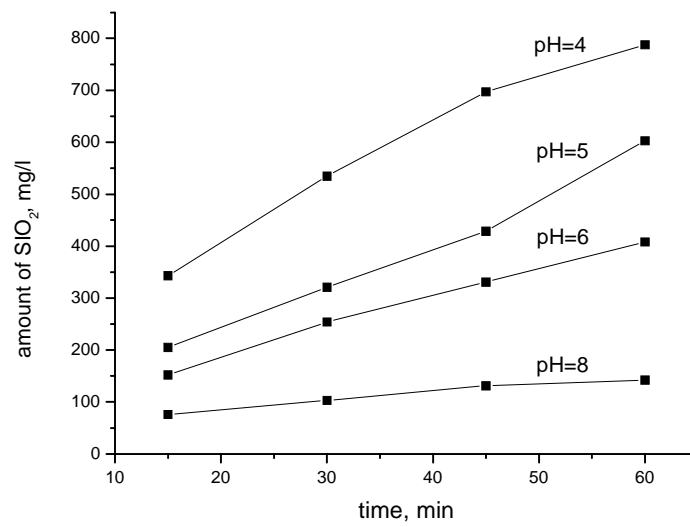
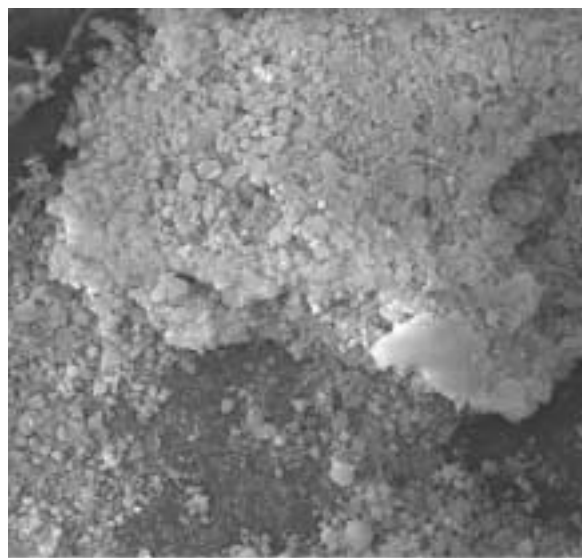
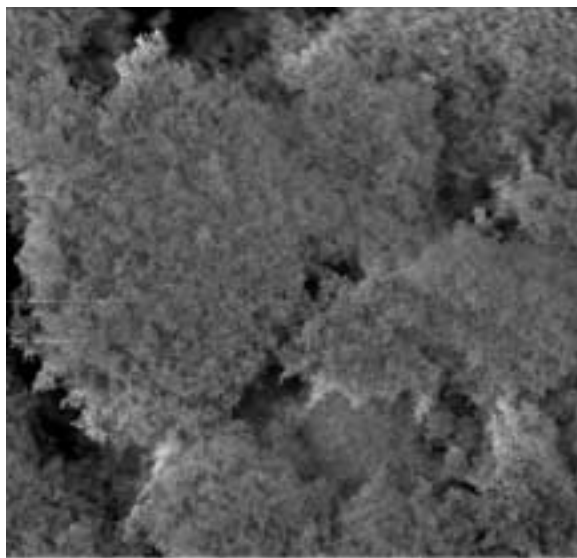


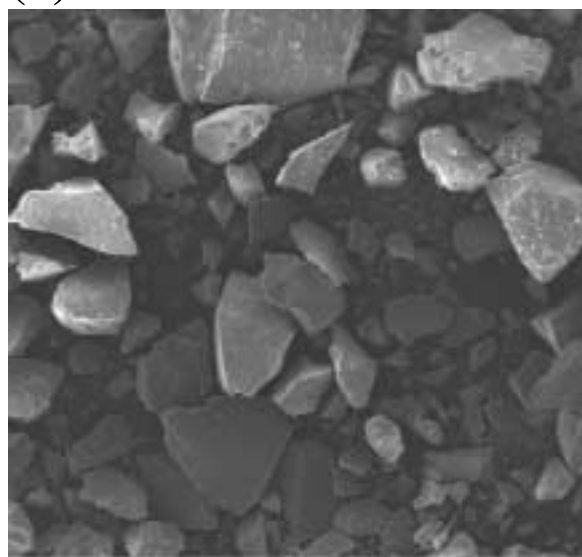
Fig. 3 Scanning electron micrographs of Aerosil 200 (a, b) and synthesized silica gel precipitated at pH = 2



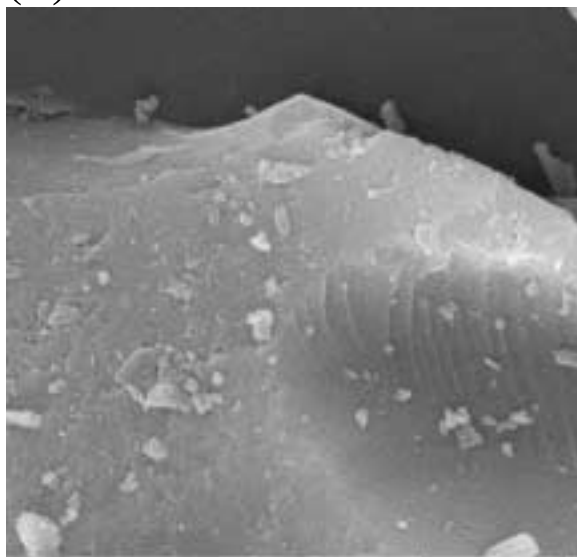
(a)



(b)



(c)



(d)

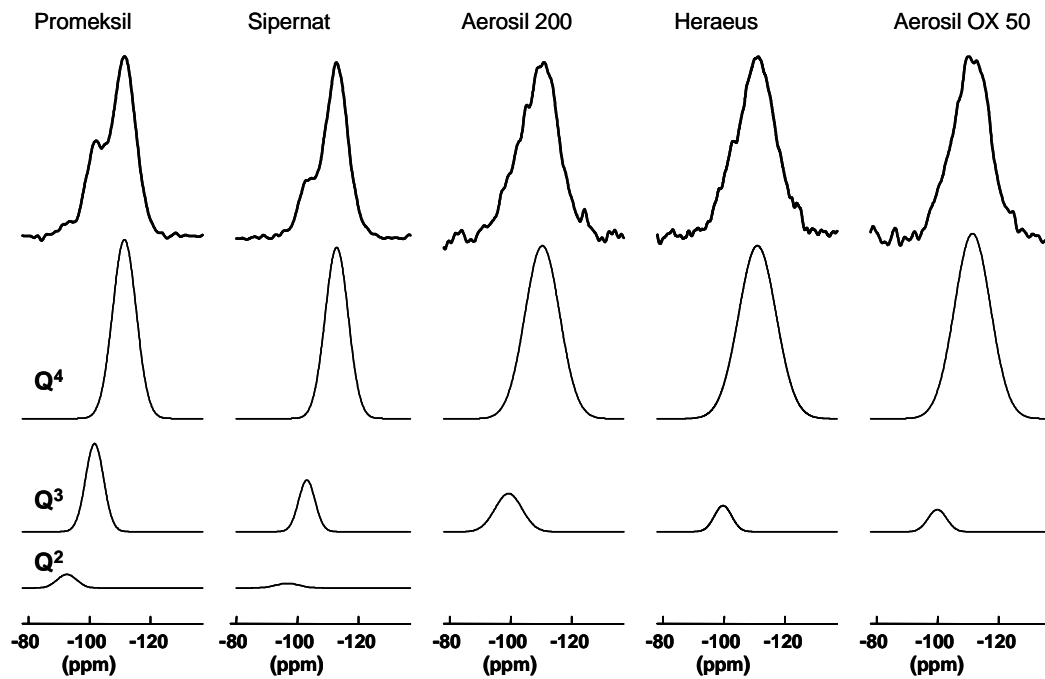
Abb. 4 ^{29}Si MAS NMR spectra of the commercial silica gels

Abb. 5 ^{29}Si MAS NMR spectra of the synthesized silica gels in dependence of the pH value

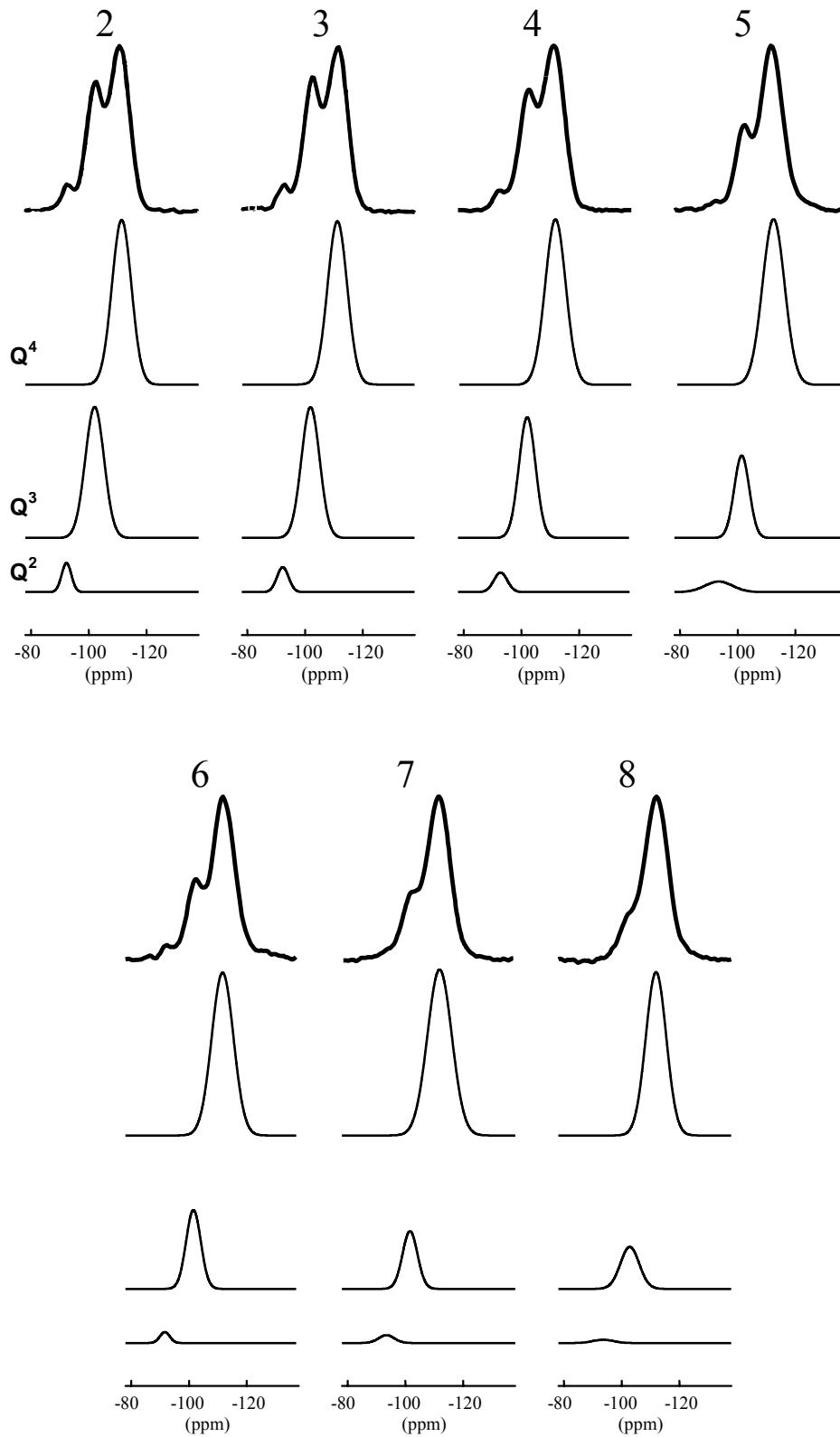
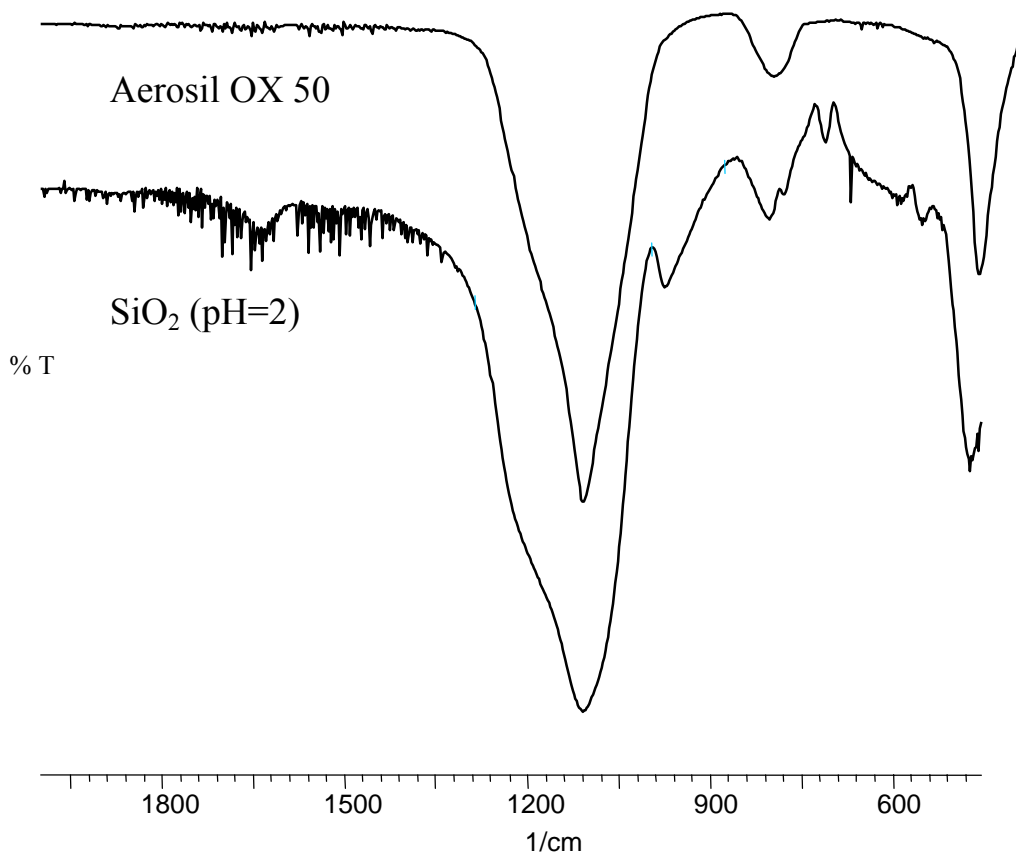


Abb. 6 IR spectra of selected commercial and synthesized silica gels



1
2
3
4
5
6
7
8
9
10
11
12
13
14
15
16
17
18
19
20
21
22
23
24
25
26
27
28
29
30
31
32
33
34
35
36
37
38
39
40
41
42
43
44
45
46
47
48
49
50
51
52
53
54
55
56
57
58
59
60

Characterization of Silica gels by ^{29}Si MAS NMR and IR Spectroscopic

Measurements

W. Lutz*, D. Täschner, R. Kurzhals, ^aD. Heidemann, ^bC. Hübert,

Berlin and Bitterfeld, Süd-Chemie Zeolites GmbH,

^aBerlin, Humboldt-Universität zu Berlin

^bCottbus, Brandenburgische Technische Universität

Received

Abstract

The solubility of commercial and synthesized silica gels in a solution of Tetra-Ethyl-Ammonium-Hydroxide (TEAOH) was investigated at room temperature. The state of parent silica frameworks was characterized by BET and SEM. The structural defects were identified both by the Q^n group analysis in ^{29}Si MAS NMR and IR spectroscopic investigation. It was found that the dissolution rate of the samples shows a tendency for growing up with an increasing BET surface. The increase of the internal surface was accompanied by formation of $\text{Si}(\text{OSi})_3(\text{OH})$ (Q^3) and $\text{Si}(\text{OSi})_2(\text{OH})_2$ (Q^2) structural units. The higher the number of Q^3 and Q^2 groups observed, the faster the samples were dissolved in TEAOH solution due to the attack of the hydroxide ions on the terminal OH groups of the framework. The asymmetrical TOT valence vibration of the IR spectra was systematically shifted to lower values with increase in the number of Q^3 and Q^2 structure groups.

1
2
3
4
5
6
7 **Keywords:** silicates, solid state structure, solvent effects, NMR spectroscopy, IR spectroscopy
8
9

10
11
12
13
14 * Wolfgang Lutz
15 Süd-Chemie Zeolites GmbH, Labor Berlin, Volmerstr. 13, 12489 Berlin
16 Tel.: 0049 30 6392 4425
17 e-mail: wolfgang.lutz@sud-chemie.com
18
19
20
21
22
23
24
25
26
27
28
29

30 Charakterisierung von Silicagelen mit Hilfe der IR- and ^{29}Si MAS NMR-
31
32
33 Spektroskopie
34
35
36
37

38 **Inhaltsübersicht.**

39
40
41 Die Löslichkeit kommerzieller Silicagele und Gele eigener Herstellung in TEAOH-Lösung
42 wurde bei Raumtemperatur untersucht. Die Löslichkeit stieg mit zunehmender Zahl von
43
44
45
46
47
48
49
50
51
52
53
54
55
56
57
58
59
60
NMR-Spektren charakterisiert wurden. Die Wellenzahl der asymmetrische TOT (T = Si)
Valenzschwingung in IR-Spektren verschob sich mit Zunahme der Strukturdefekte
systematisch zu niedrigeren Werten.

1 Introduction

Silica gels have been used in the chemical industry and laboratory technique as drying agents [1], feed stock of zeolite synthesis [2], and separation medium in chromatography [3] for a long period. More recently, they were applied also as wafer of optical sensors [4] and for heat storage by water sorption [5]. Pioneers reporting the physical and chemical properties of silica gels are Hauser [6], Sosman [7], or Hinz [8]. A general view about “The chemistry of silica” was published in 1979 by Iler [9].

Engelhardt and Michel [10] characterized the framework of silica gels by the Q^n group analysis (n = number of bridging oxygen atoms in the SiO_4 -tetrahedron under study) and Cannes [11] reported on the surface properties by the characterization of silanol groups by means of ^{29}Si MAS NMR and CP MAS NMR experiments. IR spectroscopic measurements gave information about surface OH-groups [11, 12] and the SiO_2 framework [13].

The application of silica gels for the synthesis of zeolites was described in detail by Breck [1], Barrer [2], and Zhdanov [14]. The synthesis process of these aluminosilicates follows quite different recipes. The particle size, size distribution, and shape of the crystals obtained are decisively determined by the crystallization kinetics. All parameters depend on the temperature, alkalinity and composition of the synthesis batch, and, finally, the type of silica source. While in the classical synthesis of 4A (LTA) and X (FAU) zeolites water glass solution is used as silicate component, the synthesis of zeolites beta (BEA), mordenite (MOR), or ZSM-5 (MFI) involves the silica gels.

The reactivity of silica gels depends on their solubility in the alkaline mother liquors of the synthesis batches. Mechanism, kinetics and, consequently, the quality of the final products are thereby influenced by the size of SiO_2 particles as well as by the condensation state of the SiO_2 network. The crystal shape can be characterized by the scanning electron microscopic

1
2
3 investigation (SEM) and the solubility by chemical analysis of the liquid phase. ^{29}Si MAS
4
5 NMR and IR measurements can give direct hints to the state of the SiO_2 framework.
6
7

8 This paper is aimed to demonstrate the applicability of the ^{29}Si MAS NMR as well as the IR
9
10 spectroscopy as suitable methods for the efficient characterization of the framework state of
11
12 silica gels, using two differently prepared sample series.
13
14
15
16
17
18
19
20
21
22
23
24
25
26
27
28
29
30
31
32
33
34
35
36
37
38
39
40
41
42
43
44
45
46
47
48
49
50
51
52
53
54
55
56
57
58
59
60

2 Results

The commercial and synthesized silica gels listed in Tab. 1 show similar dissolution behaviour in the TEAOH solution. The amounts of dissolved SiO_2 vary between 50 und 800 mg/l in dependence on time and sample type for both series (Figs. 1 and 2). The dissolution rate increases thereby with the absolute rising solubility of samples.

The kinetic curves of the commercial products given in Fig. 1 show higher concentrations of dissolved SiO_2 for Promeksil B12, Aerosil 200, and Sipernat 320 connected with the transformation of the solids into transparent hydrogels according to visual observation, while Silica 995 and Aerosil OX 50 show lower dissolution degree, with a formation of SiO_2 nanoparticles.

The curves of the synthesized gels in Fig. 2 demonstrate increasing dissolution with decreasing pH-values of preparation. The remaining filter cakes of this series represent white gels for all the samples.

SEM micrographs of the commercial products provide the evidence that they are composed of primary particles with a significant surface roughness. In this case, particle size distribution is broad. In contrast, the synthesized samples have somewhat greater particles with a rather smooth surface. Their size lies between 10 and 910 μm (Tab. 1). Selected replicas of both series with the typical different particle habit are shown in Fig. 3.

In opposite to the values of the particle size which does not influence the solubility of the gels in a systematic way as can be seen from Tab. 1 and Figs. 1 and 2, the BET surface of samples show a systematic change and coincides with the trend in solubility. Whereas the BET values of the commercial products vary between 42 and 413 m^2/g , the surface of the synthesized silica gels ranges from 140 to 438 m^2/g (in dependence also of sample milling). As evident from Figs. 1 and 2, the amount of dissolved SiO_2 of the Aerosil OX 50 and $\text{SiO}_2(\text{pH}=8)$ is consequently lowest and for Promeksil B12 and $\text{SiO}_2(\text{pH}=4)$ this parameter is observed as

1
2
3 being highest. Figs. 4 and 5 demonstrate this tendency by the dependence of the solubility on
4 the BET surface of samples. But in spite of the somewhat higher BET surface of the
5 synthesized gels, their solubility does not reach systematically higher values. For
6 understanding of this phenomenon, the structure of the gel frameworks must be taken into
7 consideration in more details.

8
9
10 The Q^n -group analysis on basis of the ^{29}Si MAS NMR spectroscopic measurements confirmed
11 the dependence of the gel solubility on the state of the silica framework and, thus, the
12 structure of the internal surface. The NMR spectra of the commercial silica gels in Fig. 6
13 normalized to 100% intensity show different line shapes and chemical shifts of the peaks:
14
15 Promexsil B12 and Sipernat 320 are characterized by different kinds of Q^n -signals. Firstly,
16 there is Q^4 the main signal related to each Si atom which is linked over oxygen atoms with 4
17 Si neighbours. Additional signals such as Q^3 and Q^2 are also present in this spectrum. The first
18 and the second are coming from 3 Si neighbours and 1 OH-group and 2 Si neighbours and 2
19 OH-groups, respectively. The chemical shift of the Q^4 -peak appears at about -110 ppm and
20 that of the Q^3 -peaks is observed at -100 ppm. These values of chemical shift are near to those
21 known for cristobalite rather than to tridymite or quartz. Only the Q^2 -peaks strongly differ
22 with values of -92,4 ppm and -95,3 ppm for Promexsil B12 and Sipernat 320, respectively.
23 While the Q^4 -groups characterize network with a perfect structure consisting of SiO_4 -
24 tetrahedrons, the Q^3 - and Q^2 -groups characterize an imperfect framework responsible for the
25 formation of chemically active hydroxyl groups. In this consequence, commercial Aerosil 200,
26 Silica 995 and Aerosil OX 50 contain only Q^3 -groups related to defects in decreasing extent.
27 However, their peak width is relative broad in comparison with crystalline silicate phases such
28 as quartz, tridymite, and cristobalite because of non-perfect bond length and angles of their
29 structural polyhedra. A quantification of the volume fraction of all Q -groups is shown in Tab.

30
31
32
33
34
35
36
37
38
39
40
41
42
43
44
45
46
47
48
49
50
51
52
53
54
55
56
57
58
59
60
1.

1
2
3 For all the samples except Sipernat 320, the gel solubility increases with the rising degree of
4 defects. In contrast to Silica 995, Sipernat 320 seems to be less soluble although it contains
5 quite more defects. The reason could be associated with a relative high content of Na₂O of 2.1
6 weight-% (see Tab. 1) and especially contaminants of 0.15 weight-% Al₂O₃ which remarkably
7 reduce the amount of dissolved of SiO₂. Sodium silicate and sodium aluminate which are
8 formed under action of the TEAOH solution lead to a stronger condensation of (SiO₂)_n units
9 over -Si-O-Al-O-Si- bonds. Sipernat 320 produces, therefore, more hydrogel gel than Aerosil
10 200 and Promeksil B12.
11
12

13
14
15
16
17
18
19
20
21
22 As evident from Fig. 76, ²⁹Si MAS NMR spectra of the synthesized samples show Q⁴-groups
23 as well as Q³ and Q²-groups. The corresponding signals are centred at similar chemical shifts
24 as well as Q³ and Q²-groups. The corresponding signals are centred at similar chemical shifts
25 of about -111 ppm (Q⁴), -101 ppm (Q³), and -92 to -93 ppm (Q²) as in the case of commercial
26 products. But the line width of the signals observed are smaller. This could give a hint to the
27 higher regularity in respect to the bond length and angle. This may compensate the greater
28 number of defects which affect the dissolution behaviour, therefore the solubility becomes
29 smaller than expected from the BET surface values.
30
31
32
33
34
35
36
37
38

39
40 IR spectroscopic measurements give also a direct hint to the state of the SiO₂ framework. For
41 two selected samples, typical spectra are shown in Fig. 8. One could recognise peaks for the
42 tetrahedron, the symmetrical TOT valence, and the asymmetrical TOT valence vibration in the
43 range of wave numbers of 467 to 478 cm⁻¹, 802 to 812 cm⁻¹, and 1082 to 1121 cm⁻¹,
44 respectively. Particularly, the asymmetrical TOT (T=Si) valence vibration shifts significantly
45 to lower w_{TOT} values with a raising number of the framework defects as it is shown in Tab. 1.
46
47
48
49
50
51
52
53
54
55
56
57
58
59
60
61
62
63
64
65
66
67
68
69
70
71
72
73
74
75
76
77
78
79
80
81
82
83
84
85
86
87
88
89
90
91
92
93
94
95
96
97
98
99
100
101
102
103
104
105
106
107
108
109
110
111
112
113
114
115
116
117
118
119
120
121
122
123
124
125
126
127
128
129
130
131
132
133
134
135
136
137
138
139
140
141
142
143
144
145
146
147
148
149
150
151
152
153
154
155
156
157
158
159
160
161
162
163
164
165
166
167
168
169
170
171
172
173
174
175
176
177
178
179
180
181
182
183
184
185
186
187
188
189
190
191
192
193
194
195
196
197
198
199
200
201
202
203
204
205
206
207
208
209
210
211
212
213
214
215
216
217
218
219
220
221
222
223
224
225
226
227
228
229
230
231
232
233
234
235
236
237
238
239
240
241
242
243
244
245
246
247
248
249
250
251
252
253
254
255
256
257
258
259
260
261
262
263
264
265
266
267
268
269
270
271
272
273
274
275
276
277
278
279
280
281
282
283
284
285
286
287
288
289
290
291
292
293
294
295
296
297
298
299
300
301
302
303
304
305
306
307
308
309
310
311
312
313
314
315
316
317
318
319
320
321
322
323
324
325
326
327
328
329
330
331
332
333
334
335
336
337
338
339
340
341
342
343
344
345
346
347
348
349
350
351
352
353
354
355
356
357
358
359
360
361
362
363
364
365
366
367
368
369
370
371
372
373
374
375
376
377
378
379
380
381
382
383
384
385
386
387
388
389
390
391
392
393
394
395
396
397
398
399
400
401
402
403
404
405
406
407
408
409
410
411
412
413
414
415
416
417
418
419
420
421
422
423
424
425
426
427
428
429
430
431
432
433
434
435
436
437
438
439
440
441
442
443
444
445
446
447
448
449
450
451
452
453
454
455
456
457
458
459
460
461
462
463
464
465
466
467
468
469
470
471
472
473
474
475
476
477
478
479
480
481
482
483
484
485
486
487
488
489
490
491
492
493
494
495
496
497
498
499
500
501
502
503
504
505
506
507
508
509
510
511
512
513
514
515
516
517
518
519
520
521
522
523
524
525
526
527
528
529
530
531
532
533
534
535
536
537
538
539
540
541
542
543
544
545
546
547
548
549
550
551
552
553
554
555
556
557
558
559
560
561
562
563
564
565
566
567
568
569
570
571
572
573
574
575
576
577
578
579
580
581
582
583
584
585
586
587
588
589
590
591
592
593
594
595
596
597
598
599
600
601
602
603
604
605
606
607
608
609
610
611
612
613
614
615
616
617
618
619
620
621
622
623
624
625
626
627
628
629
630
631
632
633
634
635
636
637
638
639
640
641
642
643
644
645
646
647
648
649
650
651
652
653
654
655
656
657
658
659
660
661
662
663
664
665
666
667
668
669
670
671
672
673
674
675
676
677
678
679
680
681
682
683
684
685
686
687
688
689
690
691
692
693
694
695
696
697
698
699
700
701
702
703
704
705
706
707
708
709
710
711
712
713
714
715
716
717
718
719
720
721
722
723
724
725
726
727
728
729
730
731
732
733
734
735
736
737
738
739
740
741
742
743
744
745
746
747
748
749
750
751
752
753
754
755
756
757
758
759
760
761
762
763
764
765
766
767
768
769
770
771
772
773
774
775
776
777
778
779
780
781
782
783
784
785
786
787
788
789
790
791
792
793
794
795
796
797
798
799
800
801
802
803
804
805
806
807
808
809
810
811
812
813
814
815
816
817
818
819
820
821
822
823
824
825
826
827
828
829
830
831
832
833
834
835
836
837
838
839
840
841
842
843
844
845
846
847
848
849
850
851
852
853
854
855
856
857
858
859
860
861
862
863
864
865
866
867
868
869
870
871
872
873
874
875
876
877
878
879
880
881
882
883
884
885
886
887
888
889
890
891
892
893
894
895
896
897
898
899
900
901
902
903
904
905
906
907
908
909
910
911
912
913
914
915
916
917
918
919
920
921
922
923
924
925
926
927
928
929
930
931
932
933
934
935
936
937
938
939
940
941
942
943
944
945
946
947
948
949
950
951
952
953
954
955
956
957
958
959
960
961
962
963
964
965
966
967
968
969
970
971
972
973
974
975
976
977
978
979
980
981
982
983
984
985
986
987
988
989
990
991
992
993
994
995
996
997
998
999
1000

1
2
3 units with 173 pm and 163 pm, respectively. A pure SiO₂ framework needs therefore higher
4
5 activation energy for the vibrations which reflects in a higher wave number during IR
6
7 spectroscopic measurements.
8
9

10 Although silica gels practically do not contain aluminium atoms, the shift of the TOT valence
11
12 vibration depends also on the different bond length and angle in Si(OSi)₄, Si(OSi)₃(OH) or
13
14 Si(OSi)₂(OH)₂ tetrahedra. In contrast to the synthesized samples, the w_{TOT} values of the
15
16 commercial silica gels are generally slightly higher and differ, with values ranging from 1101
17
18 to 1120 cm⁻¹ against values lying between 1082 and 1105 cm⁻¹. Taking into consideration a
19
20 sensitivity of the signals of $\pm 1\text{cm}^{-1}$ for the commercial as well as synthesized silica gels
21
22 significant changes in their structure can be observed. The results mean that commercial
23
24 products have low degree of defects which fits nicely with data obtained by the ²⁹Si MAS
25
26 NMR spectra. This is the reason why Aerosil OX 50 or SiO₂(pH=8) needs the highest and
27
28 Promexsil B12 and SiO₂(pH=2) the lowest activation energies corresponding to the highest
29
30 and the lowest IR wave numbers for each series as seen from Tab. 1. The solubility of the
31
32 samples increases in the same tendency.
33
34
35
36
37
38

39 In the series of synthesized silica gels, a specific observation lies in the fact that the saturation
40
41 of w_{TOT} begins with pH value equal to 6. In this range, the ²⁹Si MAS NMR is more sensitive
42
43 than the IR spectroscopy. Nevertheless, synthesized silica gel products could be characterized
44
45 by IR spectroscopic measurements with a high sensitivity over a wide range, too.
46
47
48
49
50
51
52
53
54
55
56
57
58
59
60

3 Discussion

The solubility of silica gels in TEAOH solution depends on the internal BET surface of samples. In opposite to crystalline porous silicates such as zeolites, the surface of silica gels with irregular pore system contains, in addition to $\text{Si}(\text{OSi})_4$ (Q^4), $\text{Si}(\text{OSi})_3\text{OH}$ (Q^3) and $\text{Si}(\text{OSi})_2(\text{OH})_2$ (Q^2) structure units. The more the SiO_2 framework is disturbed, the stronger hydroxide ions of the TEAOH solution attack the silica framework at the terminal OH groups. In the case of commercial products, manufacturing process affects the formation of structural defects and cannot be exactly estimated. In the case of silica gels which were obtained from precipitation on basis of water glass solution (synthesized samples), it was observed that the number of defects increases with decreasing the pH value during precipitation process.

The Q^n group analysis of the silica gels was successfully employed with the help of ^{29}Si MAS NMR measurements. It appeared also that IR spectroscopic analysis could help with the reliable characterization of the structure under special consideration. In this case, the asymmetrical TOT valence vibration of the SiO_2 framework shifts sensitively to lower wave numbers with the raising degree of defects.

The shape of the secondary silica gel particles, characterized by SEM, does not influence the dissolution systematically. Different residual filter cakes such as white solids, transparent hydro-gels, and silica nano-particles can be observed. The contamination of the silica gel by traces of aluminium compounds leads to the increased formation of a secondary gel phase due to precipitation of the secondary $(\text{SiO})_n$ particles containing -Si-O-Al-O-Si- bonds.

4 Experimental Part

Materials

Commercial silica gels used for different zeolite synthesis processes and shown in Tab. 1 as well as synthesized silica gels were investigated. The latter were prepared according to the following route. The aqueous solution of sodium silicate was transformed into acid silica sol using “Wofatit KPS 200” as ion exchanger resin. 220 ml silicate solution (1.8 M in SiO₂) was dropped into a stirred batch of 1000 ml resin and 200 ml water at 278 K within 10 minutes. The acidity of the as-synthesized silica sol with pH of 2 was adjusted to pH values between 3 and 8 by immediate adding of sodium hydroxide solution. SiO₂ xerogels were obtained by drying of the washed hydrogels at 383 K for 24 hours and subsequent crushing.

Solubility experiments

1 g silica gel was stirred at ambient temperature in 40 ml of a 15% aqueous solution of TEAOH for 15 – 60 minutes. Before ICP OES element analysis, the solution was separated from the solid by filtration over glass micro filters MF 100 (Fisherbrand) in a first step followed by the filtration using PTFE micro-membrans (0.2 µm) under pressure within 5 minutes. The separation period was part of the total treatment time. The solubility of the glass filter material does not exceed 3 mg/l and can be, therefore, neglected. Cellulose membranes were non-suitable for the separation procedure because the material dissolves itself under these conditions.

The filtrates were analyzed by use of a IRIS Intrepid High Resolution spectrometer (Thermo Elemental, USA). The ICP OES was calibrated within reference to synthesized solution standards. The accuracy of the measurements lies around 1-3 % within relative standard deviation (RSD) for values above background equivalent concentration (BEC).

Characterization of xerogels

The ^{29}Si MAS NMR spectra were recorded at room temperature on a Bruker Avance 400 spectrometer, operating at frequencies of 79.5 MHz. A 4 mm double tuned (^1H -X) MAS probe (Bruker Biospin) was used to perform MAS NMR measurements at spinning rates of 12 kHz. The spectra were obtained with a single pulse excitation consisting of 4 μs pulses ($\pi/2$ pulses) and recycle delays of 120 seconds to exclude saturation effects. Measurements in the high power decoupling mode (HPDEC) brought no higher resolution of the signals. Up to 700 FIDs were accumulated to obtain reliable signal-to-noise ratio. The spectra were externally referenced to liquid Me_4Si at 0 ppm. A detailed Q^n -group characterization includes the line shape analysis of the NMR spectra by use of an iterative deconvolution procedure with the help of dmfit software package [15].

IR absorption spectra were taken on a Shimadzu FTIR 8400S spectrometer with a resolution of $\pm 1 \text{ cm}^{-1}$ by use of 30 scans. For analysis, 0.5 mg of the sample was pressed with 400 mg KBr into a pellet and measured in the IR range of 400 cm^{-1} to 4000 cm^{-1} .

Scanning electron microscopy (SEM) was performed on a Hitachi S2400 with W cathode at the accelerating potential of 15-20 kV. To produce the conductive layer, the particles were sputtered by a thin gold coating.

Chemical element analysis was measured by using XRF spectrometer PW2404 from Panalytical. 0,5 g of the sample were fused with 3 g lithium borate ($\text{Li}_4\text{B}_6\text{O}_{11}$ - Spectromelt A12 from Merck GmbH) in a platinum crucible to cast a 27 mm diameter glass disc.

The BET surface area was determined on basis of the volumetric nitrogen adsorption at $p/p_0 = 0.075, 0.1, \text{ and } 0.125$ at -77.8 K on a Nova 1200 of the Quantachrome Corporation.

References

- [1] D.W. Breck, *Zeolite Molecular Sieves*, John Wiley & Sons, London, 1974.
- [2] R. Barrer, *Hydrothermal Chemistry of Zeolites*, Academic Press, London, 1982.
- [3] E. Leibnitz, H. G. Struppe, *Handbuch der Gaschromatographie*, Akademische Verlagsanstalt, Leipzig, 1984.
- [4] C. Mc Donagh, P. Bowe, K. Mongey, B. D. Mac Craith, *J. Non-Cryst. Solids*, **2002**, 306, 138.
- [5] A.O. Dieng, R.Z. Wang, *Renew. Sustainable Energy Rev.*, **2001**, 5, 313.
- [6] E. H. Hauser, *Silicic Science*, Van Nostrand, Princeton, 1955.
- [7] R. B. Sosman, *The Phase of Silica*, Rutgers University Press, New Brunswick, 1965.
- [8] W. Hinz, *Silicate: Grundlagen der Silicatwissenschaft und Silicattechnik*, Vol. 2, Verlag Bauwesen, Berlin, 1971.
- [9] R.K. Iler, *The chemistry of silica*, Wiley & Sons, New York, 1979.
- [10] G. Engelhardt, D. Michel, *High Resolution Solid State NMR of Silicates and Zeolites*, Wiley & Sons, New York, 1987.
- [11] C. Cannas, M. Casu, A. Musinu, G. Piccaluga, *J. Non-Cryst. Solids*, **2005**, 351, 3476.
- [12] J. Estella, J. C. Echeverria, M. Laguna, J. Garrido, *Microp. Mesopor. Mater.*, **2007**, 102, 274.
- [13] A. Fidalgo, L. M. Ilharco, *Microp. Mesopor. Mater.*, **2005**, 84, 229.
- [14] S.P. Zhdanov, S.S. Chvoshchev, N.N. Samulevich, *Synthesized Zeolites*, Gordon & Breach Science Publishers, New York, 1990.
- [15] D. Massiot, F. Fayon, M. Capron, I. King, S. Le Calvé, B. Alonso, J.O. Durand, B. Bujoli, Z. Gan, G. Hoatson, *Magn. Reson. Chem.* 40 (2002) 70 - 76
- [16] E. M. Flanigen, in *Zeolite Chem. Catal.* Ed. J. A. Rabo, ACS Monographs 171 (1976) 81.

- 1
2
3 [17] H. Fichtner-Schmittler, U. Lohse, H. Miessner, H. E. Maneck, *Z. Phys. Chem.*
4
5 Leipzig 271 (1990) 69.
6
7
8 [18] C. H. Rüscher, J.-Chr. Buhl, W. Lutz, in A. Galarneau, F. Di Renzo, F. Fajula, and
9
10 J. Vedrine (Eds.), *Stud. Surf. Sci. Cat.*, Vol. 135, Elsevier, Amsterdam, 2001, 13-P15,
11
12 p. 1.
13
14
15
16
17
18
19
20
21
22
23
24
25
26
27
28
29
30
31
32
33
34
35
36
37
38
39
40
41
42
43
44
45
46
47
48
49
50
51
52
53
54
55
56
57
58
59
60

Table 1 Chemical and physical data of used commercial and synthesized silica gels

sample denotation	sample type	particle size ¹ μm	BET surface m ² /g	IR ν_{TOT} , cm ⁻¹	portion of Q ⁴	²⁹ Si MAS of Q- Q ³	NMR groups, % Q ²
<i>commercial silica gels</i>							
Promexsil B12	precipitated	≤ 10	413	1101	70	26	4
Sipernat 320	precipitated	≤ 75	196	1107	80	17	3
Aerosil 200	pyrogene	≤ 310	210	1110	85	15	0
Silica 995	pyrogene	≤ 28	61	1117	93	7	0
Aerosil OX 50	pyrogene	≤ 34	42	1120	94	6	0
<i>synthesized silica gels</i>							
SiO ₂ (pH 2)	precipitated	≤ 380	538	1082	54	41	5
SiO ₂ (pH 3)	precipitated	≤ 285	513	1088	56	39	5
SiO ₂ (pH 4)	precipitated	≤ 105	507	1095	61	34	5
SiO ₂ (pH 5)	precipitated	≤ 95	404	1101	71	24	5
SiO ₂ (pH 6)	precipitated	≤ 110	352	1105	74	24	2
SiO ₂ (pH 7)	precipitated	≤ 910	172	1103	81	17	2
SiO ₂ (pH 8)	precipitated	≤ 115	140	1105	80	19	1

¹ estimated from SEM with an error of ± 5%

Fig. 1 Alkaline solubility of commercial silica gels in dependence on time

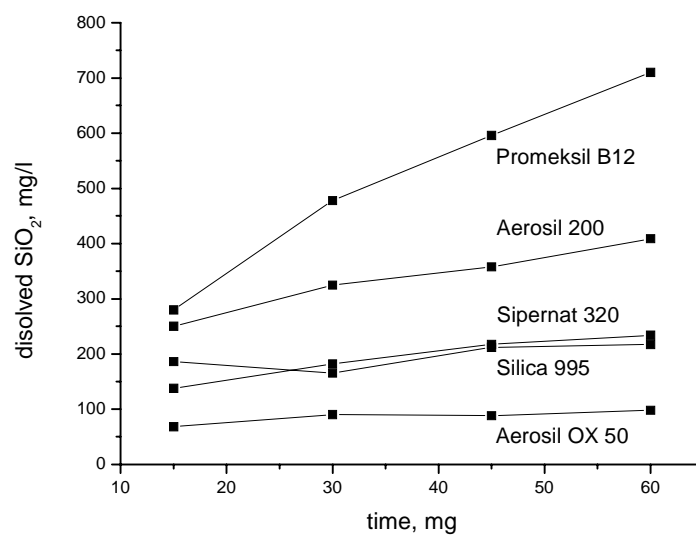


Fig. 2 Alkaline solubility of synthesized silica gels in dependence on time

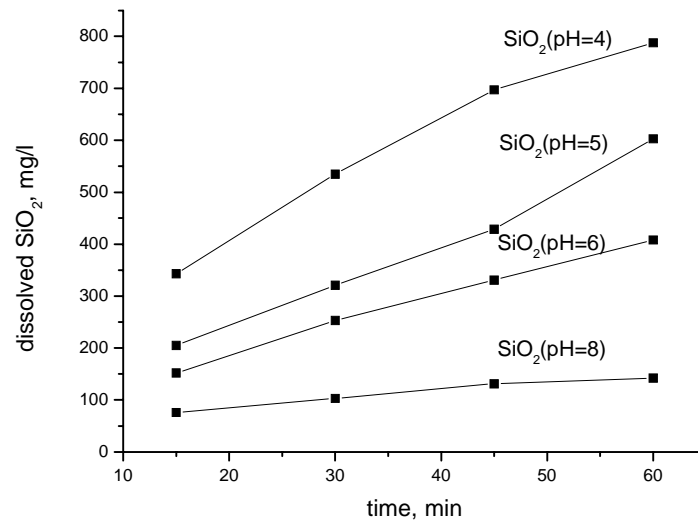
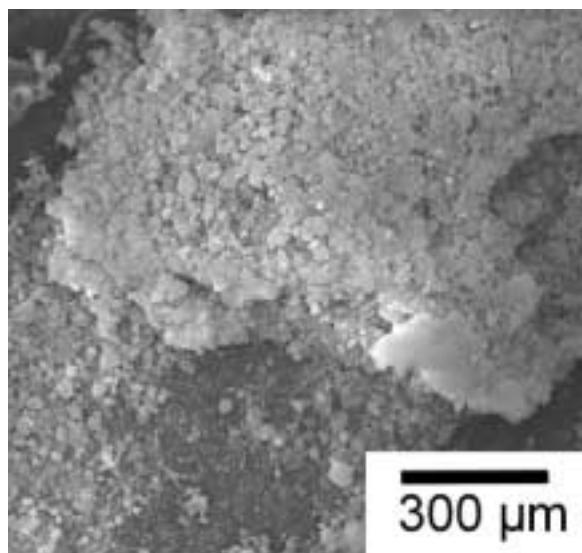
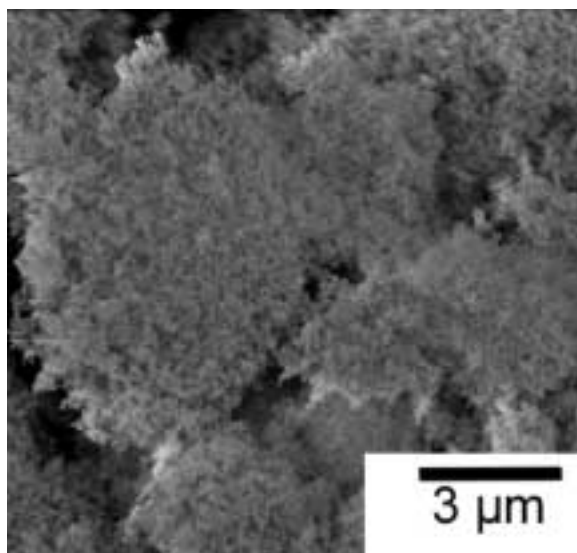


Fig. 3 Selected scanning electron micrographs of a commercial (Aerosil 200 - a, b) and a synthesized silica gel ($\text{SiO}_2(\text{pH}=2)$ - c, d) with typical different particle habit

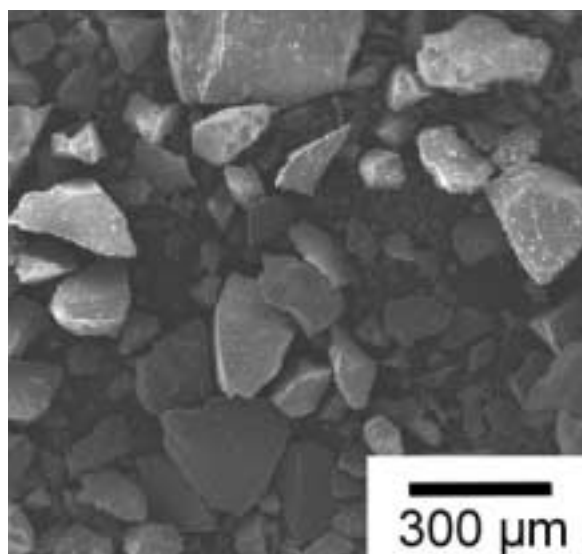
(a)



(b)



(c)



(d)

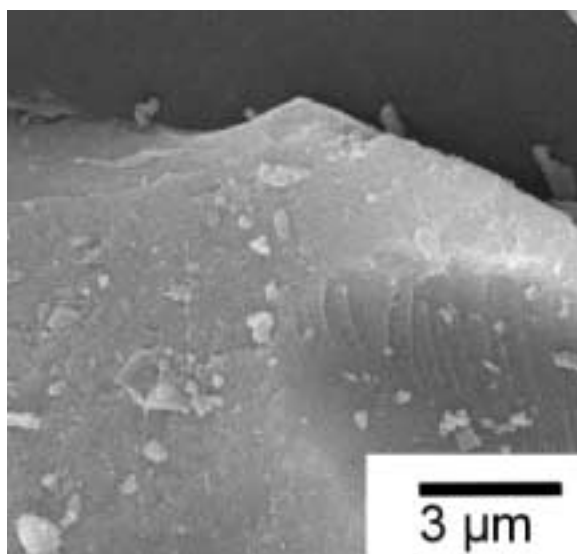


Fig. 4 Influence of the BET surface on the alkaline solubility of commercial silica gels after 60 min stirring

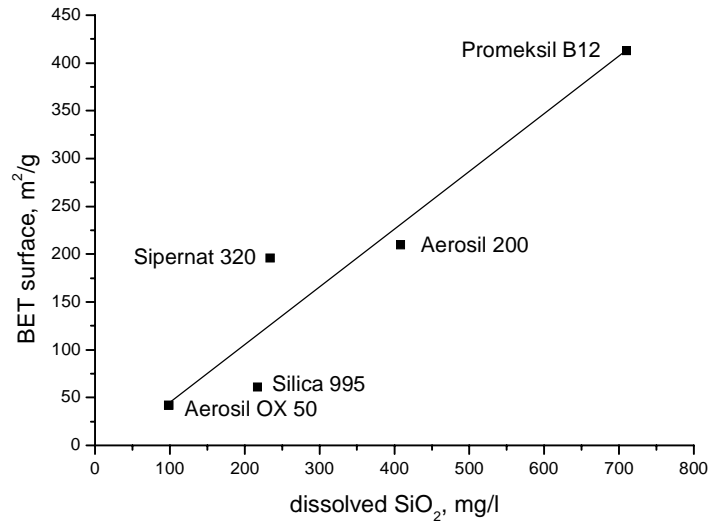


Fig. 5 Influence of the BET surface on the alkaline solubility of synthesized silica gels after 60 min stirring

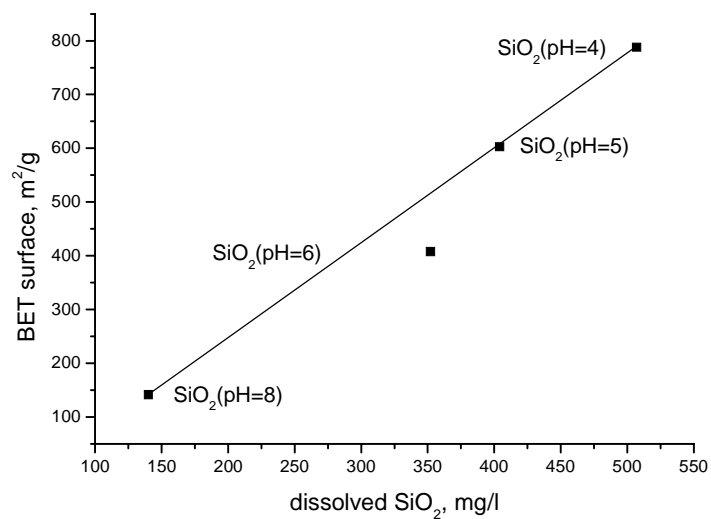


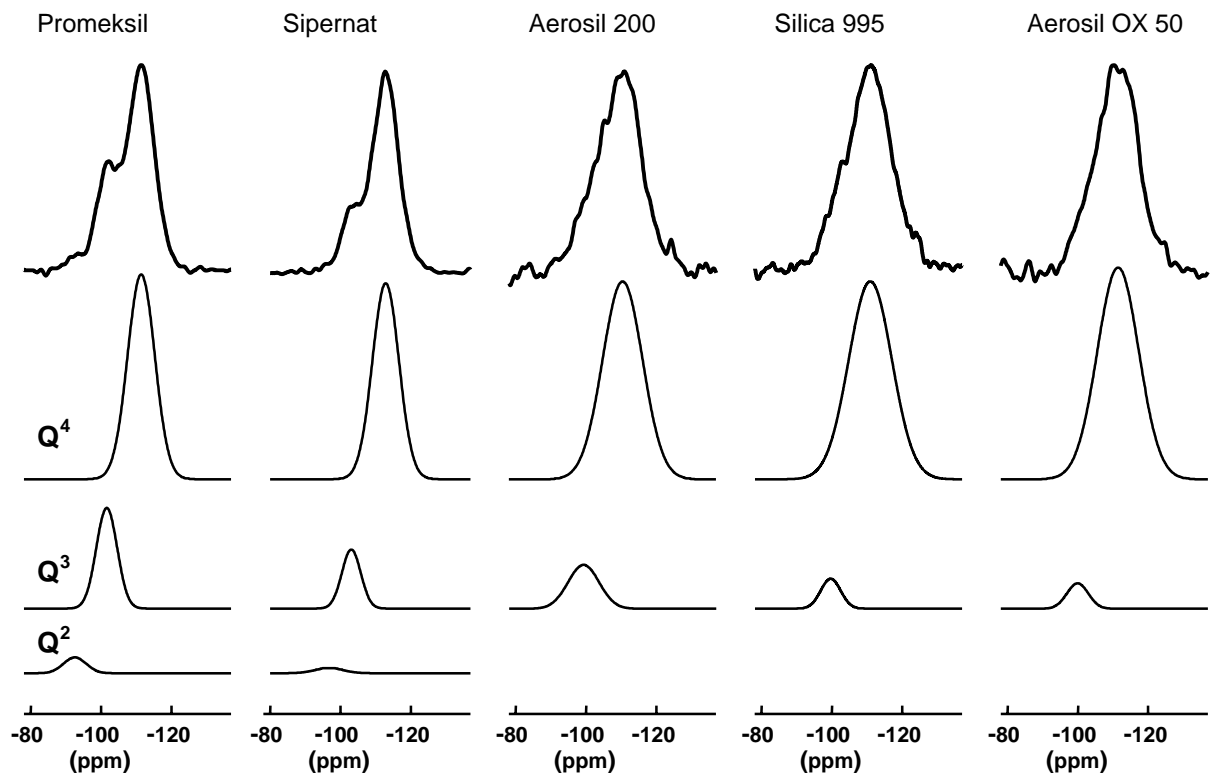
Abb. 6 ^{29}Si MAS NMR spectra of the commercial silica gels

Abb. 7 ^{29}Si MAS NMR spectra of the synthesized silica gels in dependence of the pH value

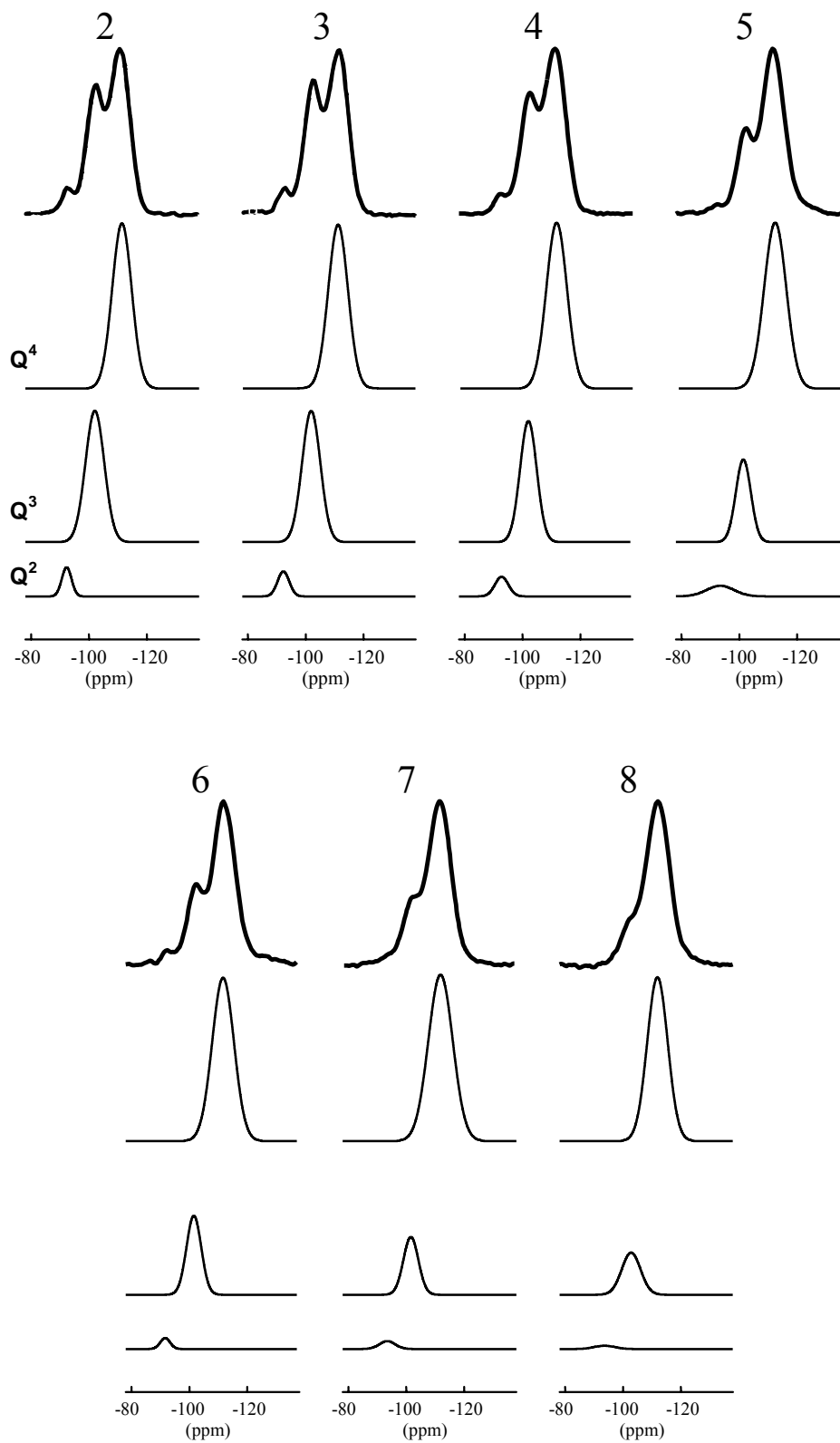


Abb. 8 IR spectra of two selected commercial and synthesized silica gel samples

